Portable low-coherence interferometer for quantitative phase microscopy of live cells

Natan T. Shaked and Pinhas Girshovitz
Department of Biomedical Engineering, Faculty of Engineering,
Tel Aviv University, Ramat Aviv 69978, Israel

ABSTRACT

We present a compact, highly portable and inexpensive interferometric module for obtaining spatial interferograms of microscopic biological samples, without the strict stability and the highly-coherent illumination that are usually required for interferometric microscopy setups. The module is built using off-the-shelf optical elements and can easily operate with low-coherence illumination, while being positioned in the output of a conventional transmission microscope. The interferograms are processed into the quantitative amplitude and phase profiles of the sample. Based on the phase profile, the optical thickness or optical path delay profile of the sample is obtained with temporal and spatial stabilities, at the order of 0.2-0.3 nm. We show several configurations of this interferometer that are suitable for both on-axis and off-axis holographic geometries, and present various experimental results, including imaging live cells in a non-contact label-free manner and transparent elements with nano-scale thickness. Since the interferometer can be connected to the output of a transmission microscope and operate in a simple way, without involvement of an expert user with a knowledge in optics and without complicated alignment prior to every experiment, and still obtain a remarkably high accuracy, we believe that this new setup will make interferometric phase microscopy more accessible and affordable for biologists and clinicians, while significantly broadening its range of applications.

Keywords: Holographic microscopy, Interferometric microscopy, Live cell quantitative imaging.

1. INTRODUCTION

Wide-field interferometric phase microscopy (IPM), also known as digital holographic microscopy, is a label-free powerful tool that is utilized for a wide range of applications including live cell quantitative imaging [1-4]. IPM is able to capture the optical thickness or optical path-delay map of the sample and track sub-nanometric changes occurring in it, with acquisition frame rates of up to several thousands of full frames per second.

IPM uses interference to record the complex wave front (amplitude and phase) of the light interacted with the sample. For biological and medical applications, the ability to record the sample quantitative phase enables the user to see cells and organisms, which are otherwise transparent due to the low absorption and scattering of the light transmitted through the cells. This is done without using contrast agents (such as fluorescent dyes), without contact with the sample, and without the need for scanning. Yet, the optical thickness profile obtained is quantitative, meaning that it is possible to obtain the optical thickness for each point on the sample, and using this profile, one can calculate various cell parameters such as dry mass, volume and rigidity map of the cells [1,3,4].

Wide-field IPM could be widely used for clinical applications due to its unique advantages. However, at this point, there are not many options for commercial interferometric microscopes compared to other microscopy techniques, and therefore this tool is mostly used by optical and biomedical engineers for research purposes. The main reason for this is the difficulty to obtain high-quality and stable interference patterns with modest and portable equipment, and without the need for an expert user.

To solve this problem, our group has suggested the τ interferometer [5,6], a compact, portable and inexpensive device that can be connected to the output of a transmission microscope and obtain spatial interferograms of microscopic samples, without the strict stability and the highly-coherent illumination that are usually required for interferometric microscopy setups. The device is built using off-the-shelf optical elements and can easily operate with low-coherence illumination without extensive optical knowledge or the need for meticulous alignment prior to every experiment. Still, due to its common-path, low-coherence design, this simple device can measure the optical thickness profile with temporal and spatial stabilities at the order of 0.2-0.3 nm, which is even better compared to larger, bulky and much more expensive IPM setups.

Three-Dimensional and Multidimensional Microscopy: Image Acquisition and Processing XX,
edited by Carol J. Cogswell, Thomas G. Brown, Jose-Angel Conchello, Tony Wilson, Proc. of SPIE Vol. 8589,
858913 · © 2013 SPIE · CCC code: 1605-7422/13/$18 · doi: 10.1117/12.2001758

2. OPTICAL SETUP

Figure 1 shows the τ interferometer setup in on-axis geometry (Fig. 1(a)) [5] and in off-axis geometry (Fig. 1(b)) [6]. In the on-axis τ interferometer (Fig. 1(a)), the image plane in the output of the microscope is Fourier transformed by lens L1, while being split into two beams using a beam splitter. One of the beams (defined as the sample beam) is reflected by the mirror M1 and then Fourier transformed back to the camera plane using lens L2, whereas the other beam (defined as the reference beam) is spatially filtered by pinhole P, reflected by mirror M2, and Fourier transformed back to the camera plane by lens L2. The spatial filtering effectively creates a reference beam by erasing the sample information from one of the beams, and thus enables quantitative interference on the camera. Using a pinhole in the reference beam path also increases the beam spatial coherence. In this setup, the two beams are on the same optical axis, causing the beams to propagate in the same direction after L2 lens. This setup generates, in principle, an on-axis interference pattern on the digital camera, which reduces the dynamic capabilities of this setup, since in this case several phase-shifted interferograms are required for the reconstruction process. To reconstruct the sample profile using one interferogram, one can shift the camera to the edge of the interference pattern so that an off-axis interferogram appears on a small area where the fringes are parallel straight lines. However, this can be obtained in a very limited field of view, and thus the sample size that can be recorded is significantly reduced.

To solve these problems, we lately proposed the off-axis τ interferometer [6], which is an important modification on the previously proposed τ interferometer. Figure 1(b) presents the newly proposed off-axis τ interferometer, which is able to create a full off-axis interference pattern on the camera. In order to create an angle between the sample beam and the reference beam, and enable an off-axis interferogram, the actual Fourier plane center, described by the continuation of the reflected beam (blue lines in Fig. 1(b)), is shifted using retro-reflector RR. This retro-reflector is built using a pair of mirrors attached to each other in a right angle.

To demonstrate the operation of the τ interferometer, we have constructed the experimental setup illustrated in Fig. 2. This setup contains an invert microscope with a single 40×, 0.66-numerical-aperture, infinity-corrected microscope objective, spherical tube lens with 15 cm focal length, and a monochromatic CMOS camera with 5.2 μm square pixels (DCC1545M, Thorlabs). The on-axis or off-axis τ interferometers described above were connected between the microscope camera port and the digital camera.

The light source used in the input of the invert microscope is a supercontinuum fiber-laser source (SC400-4, Fianium), connected to a computer-controlled acousto-optical tunable filter (SC–AOTF, Fianium), tuned to a central

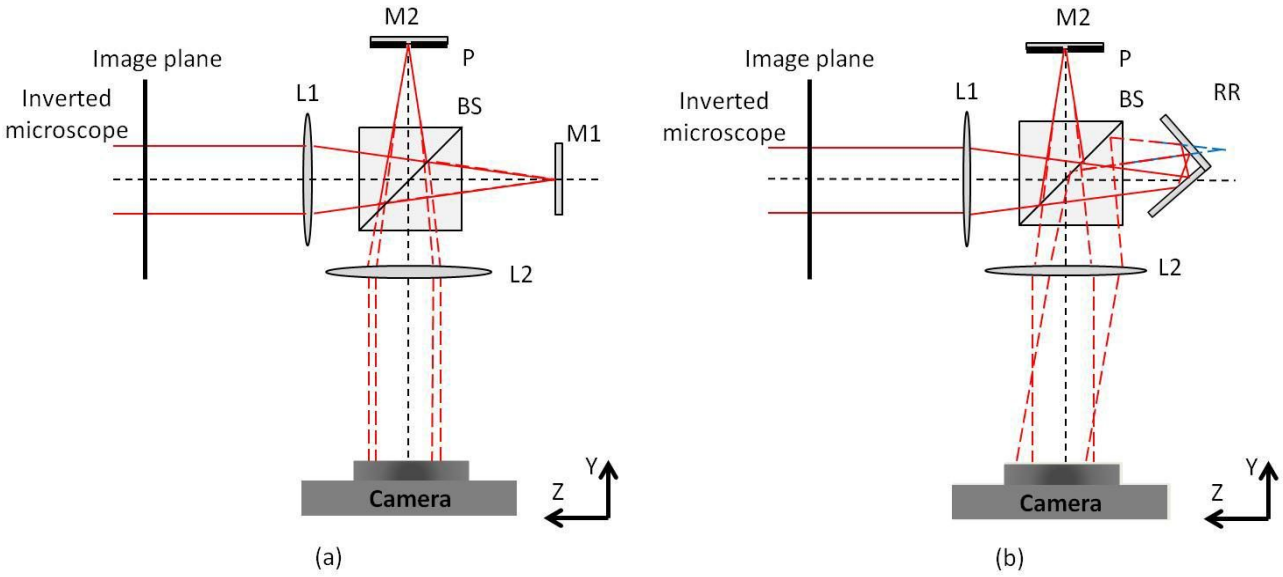

Fig. 1. Schematic system diagrams of: (a) the on-axis τ interferometer [5]; (b) the off-axis τ interferometer [6]. L1,L2 – lenses in a 4f configuration, BS – beam splitter, M1,M2 – mirrors, P – pinhole, RR – retro-reflector made of a two-mirror construction. Figure is taken from Ref. [6]. Optical Society of America, 2013(c).

wavelength of 633 nm and a full-width-at-half- maximum bandwidth of 6.7 nm, as measured by a compact spectrometer (USB4000-VIS-NIR, Ocean Optics), leading to a coherence length of 26.4 μm. Note that the condenser lens was removed from the inverted microscope so that we can compare the performance of the system with other conventional IPM setups which use plane-wave illumination. In spite of this, as confirmed experimentally, the proposed interferometric setup can also operate when the inverted microscope uses a condenser lens, while improving the spatial resolution of the microscope and better using the numerical aperture of the objective lens.

Note that only simple optical elements and no gratings or other diffractive elements are used inside the interferometric system, in contrast to the setup proposed in Refs. [7-9]. In addition, there is no limitation on the confluence of the sample (thus, we do not need to use half-empty sample), in contrast to other setups [10,11].

Using this device is simple and straightforward: the user is only expected to place the sample on the regular microscope stage, without any preparations or using fluorescent labeling and without difficult alignment procedures. The user should ensure that the expected varying thickness of the sample do not exceed the temporal coherence length of the light source used. The user is not required considering the thickness of constant or slowly varying elements in the optical path such as the cover slips and cell media due to the fact that the optical thicknesses of these elements are still encoded into the reference beam, even after passing through the pinhole [6].

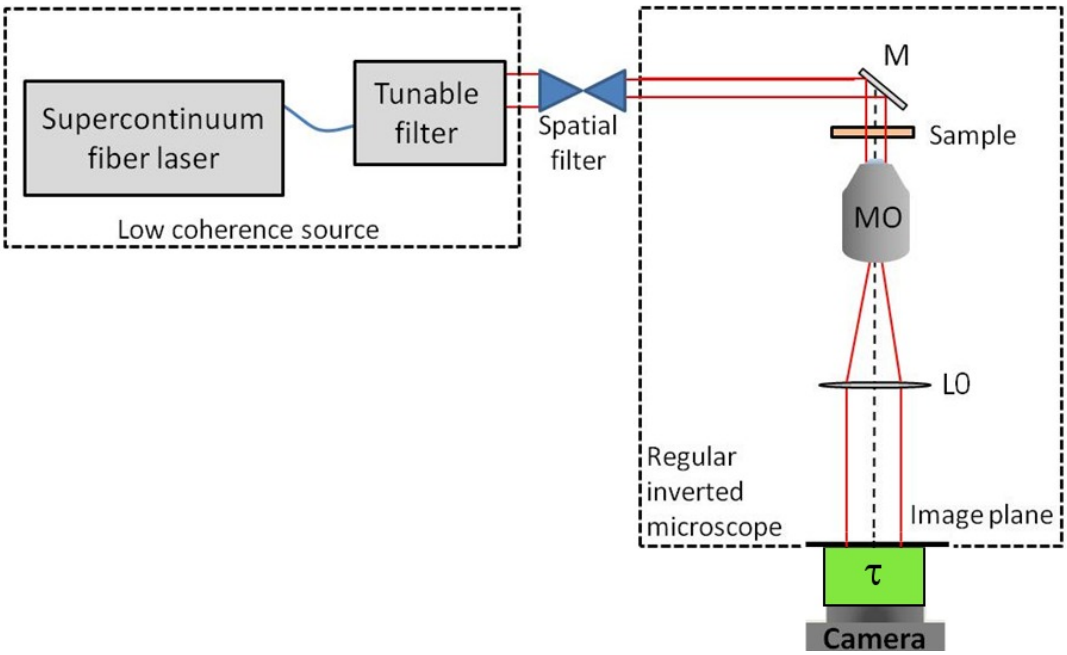

Fig. 2. The τ interferometer (green box in front of the camera), connected in the output of an inverted microscope, which is illuminated by a tunable low-coherence source. MO – microscope objective, L0 – lens, M mirrors, τ – one of the on-axis or off-axis τ interferometers illustrated in Fig. 1.

3. EXPERIMENTAL RESULTS

We acquired 100 interferograms per second and processed them into the phase profile of the sample by using a digital spatial filtering of a cross-correlation term from the other terms [6], followed by subtraction of the phase profile obtained from an interferogram without the presence of the specimen, which compensates for phase aberrations introduced by the system [6], and a phase unwrapping algorithm for removing 2π ambiguities [12].

We first estimate the setup spatial and temporal noise levels, which determine the optical thickness sensitivity across an image and between images, respectively. The spatial noise level was found to be 0.42 nm in the on-axis τ interferometer and 0.35 nm in the off-axis τ interferometer, whereas the temporal noise level was found to be 0.18 nm in the on-axis τ interferometer and 0.28 nm in the off-axis τ interferometer. For comparison, a conventional Michelson

interferometer under the same conditions (without using an enclosure) obtained temporal noise of 2.4 nm and spatial noise of 3.8 nm.

Figure 3 shows the thickness profile of a human red blood cell obtained from a single single-exposure interferogram using the on-axis τ interferometer and the low-coherence light source. To obtain the cell thickness profile, we divided the optical thickness profile of the cell by the difference between the refractive index of the cell (n = 1.395), under the assumption of homogenous refractive index for an enucleated red blood cell [13,14], and the refractive index of the surrounding media (n = 1.34). As shown in this figure, due to the use with a low-coherence source, the background around the red blood cell (containing only cell media) is remarkably flat, with a standard deviation of spatially-averaged optical path delay of 0.85 nm in liquid environment. Note that this image was obtained when we shifted the camera field of view to the edges of the interference pattern to obtain off-axis interference. This off-axis interference can be obtained in a very limited field of view.

As shown in Fig. 4, this limitation is solved by using the off-axis τ interferometer, which can obtain off-axis interference on a much wider field of view, limited only by the coherence length of the source.

In Ref. [6], we also imaged two phase targets that were designed in the computer and then generated by a focused ion beam (FIB) lithography. FIB lithography operates in a similar fashion of a scanning electron microscope (SEM) but rather uses a finely focused gallium beam. FIB is capable of milling the surfaces of substrates and creating nanometer-scale-topography phase targets [15]. Using FIB lithography, we created several shapes on a chrome-plated glass

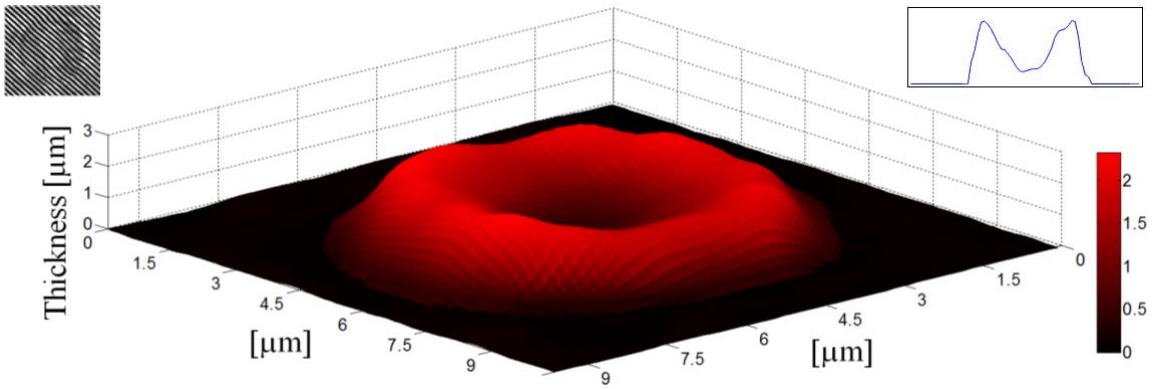

Fig. 3. Quantitative thickness profile of a red blood cell acquired with the on-axis τ interferometer, when shifted to the edge of the on-axis interference pattern. Colorbar represents thickness in μm. Left inset: interferogram of a single red blood cell, obtained on a limited field of view. Right inset: cross-section across the cell diagonal (marked by arrows). Figure is taken from Ref. [5]. Optical Society of America, 2012(c).

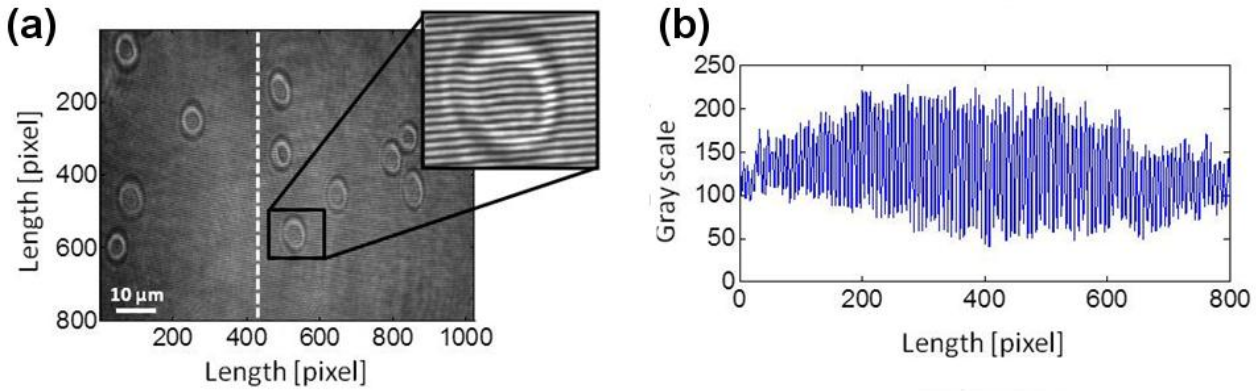

Fig. 4. (a) Off-axis interferogram of red blood cells, obtained by the off-axis τ interferometer on a significantly wider field of view compared to this obtained by the on-axis τ interferometer. (b) A cross-section along the white dashed line in the interferogram shown in (a). Figure is taken from Ref. [6]. Optical Society of America, 2013(c).

coverslip (10 nm plating) in different heights. One of these optically transparent targets contained the words "OMNI Group" with a line width of 0.7 μm (close to the microscope diffraction-limit spot) and an optical thickness of 20 nm (10 nm due to the milling of the chrome and 10 nm due to the milling of the glass). Figure 5 presents the optical thickness map of this target as obtained by the off-axis τ interferometer using a low-coherence source (Fig. 5(a)), by the off-axis Mach-Zehnder interferometer using a low-coherence source (Fig. 5(b)), and by the Mach-Zehnder interferometer using a high-coherence source (Fig. 5(c)).

In Fig. 5(a), the lithographed text "OMNI Group" is clearly seen and distinguished from the background, whereas in the measurements done by the off-axis Mach-Zehnder interferometer, presented in Figs. 5(b,c), the background noise level conceals most of the lithographed text and only several lines are barely seen. In this demonstration, it is clearly seen that due to the lower spatial noise level of the off-axis τ interferometer, it is possible to image smaller features that the other conventional IPM setups cannot see.

The average optical thickness of the lithographed text letters was calculated as 19.4 nm (n_{chrome} =2.42 and n_{glass} =1.515). Note that minimal milling capability of the FIB setups used by us is 10 nm, so it is possible that the inconstant optical thickness of the letters seen in Fig. 5(a) is caused by the milling process of the glass layer and not due to the spatial interferometric noise. In any case, these results show that the off-axis τ interferometer can also be used to perform inexpensive quality checks and imaging during the manufacturing of transparent optical elements, as long as the lateral dimensions of the smallest element that needs to be examined is larger than the diffraction-limit spot of the microscope.

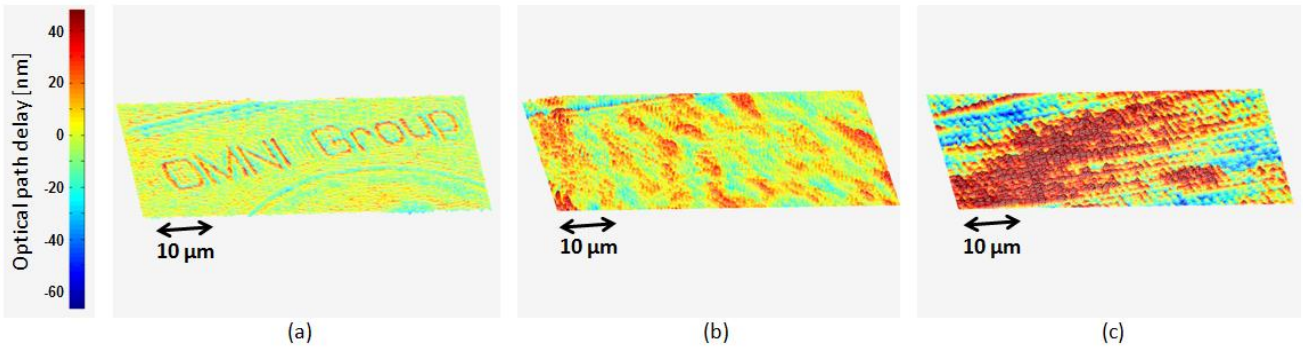

Fig. 5. Optical thickness or optical path delay maps of the second phase target created by FIB lithography, containing variable depth elements, as obtained using: (a) off-axis τ interferometer with a low-coherence source; (b) off-axis Mach-Zehnder interferometer with a low-coherence source; and (c) off-axis Mach-Zehnder interferometer with a high-coherence source (HeNe laser). Figure is taken from Ref. [6]. Optical Society of America, 2013(c).

4. CONCLUSIONS

In conclusion, we have presented the τ interferometer, a compact, portable, and extremely stable common-path interferometric setup that enables recording the amplitude and the phase profiles of biological samples using a low-coherence source, without the need for special optical elements and an expert alignment prior to every experiment. We presented the off-axis and on-axis interferometric geometries for this device.

We expect that in mass production, the τ interferometer size can be reduced to a cube of 1-3 inch length (depending on the chosen geometry), with total cost of less than $500. Due to its low cost and simple design and operation, we expect that this portable off-axis interferometer will make wide-field IPM measurements more common for clinical diagnosis, for biological research and for nondestructive testing in the industry.

REFERENCES

[1] Rappaz, B., Barbul, A., Emery, Y., Korenstein, R., Depeursinge, C., Magistretti, P. J., and Marquet, P., "Comparative study of human erythrocytes by digital holographic microscopy, confocal microscopy, and impedance volume analyzer," Cytometry A 73A, 895–903 (2008).

[2] Kemper, B., Bauwens, A., Vollmer, A., Ketelhut, S., Langehanenberg, P., Müthing, J., Karch, H., and Bally, G., "Label-free quantitative cell division monitoring of endothelial cells by digital holographic microscopy," J. Biomed. Opt. 15, 036009 (2010).

[3] Shaked, N. T., Satterwhite, L. L., Truskey, G. A., Telen, M. J., and Wax, A., "Quantitative microscopy and nanoscopy of sickle red blood cells performed by wide field digital interferometry," J. Biomed. Opt. 16, 030506 (2011).

[4] Girshovitz, P. and Shaked, N. T., "Generalized cell morphological parameters based on interferometric phase microscopy and their application to cell life cycle characterization," Biomed. Opt. Express 3, 1757–1773 (2012).

[5] Shaked, N. T., "Quantitative phase microscopy of biological samples using a portable interferometer," Opt. Lett. 37, 2016–2019 (2012).

[6] Girshovitz, P. and Shaked, N. T., "Compact and portable low-coherence interferometer with off-axis geometry for quantitative phase microscopy and nanoscopy," Accepted to Opt. Express (2013).

[7] Monemhaghdoust, Z., Montfort, F., Emery, Y., Depeursinge, C., and Moser, C., "Dual wavelength full field imaging in low coherence digital holographic microscopy," Opt. Express 19, 24005–24022 (2011).

[8] Popescu, G., Ikeda, T., Dasari, R. R., and Feld, M. S., " Diffraction phase microscopy for quantifying cell structure and dynamics," Opt. Lett. 31, 775-777 (2006).

[9] Kolman, P. and Chmelík, R., "Coherence-controlled holographic microscope," Opt. Express 18, 21990–22003 (2010).

[10] Jang, J., Bae, C. Y., Park, J. K., and Ye, J. C., "Self-reference quantitative phase microscopy for microfluidic devices," Opt. Lett. 35, 514–516 (2010).

[11] Kemper, B., Vollmer, A., Rommel, C. E., Schnekenburger, J., and Bally, G., "Simplified approach for quantitative digital holographic phase contrast imaging of living cells," J. Biomed. Opt. 16, 026014 (2011).

[12] Ghiglia, D. C. and Pritt, M. D., [Two-Dimensional Phase Unwrapping: Theory, Algorithms, and Software], Wiley, (1998).

[13] Park, Y. K., Diez-Silva, M., Popescu, G., Lykotrafitis, G., Choi, W., Feld, M. S., and Suresh, S., "Refractive index maps and membrane dynamics of human red blood cells parasitized by Plasmodium falciparum," Proc. Natl. Acad. Sci. U.S.A. 105, 13730–13735 (2008).

[14] Shock, I., Barbul, A., Girshovitz, P., Nevo, U., Korenstein, R., and Shaked, N. T., "Optical phase measurements in red blood cells using low-coherence spectroscopy," J. Biomed. Opt. 17, 101509 (2012).

[15] Reyntjens, S. and Puers, R., "A review of focused ion beam applications in microsystem technology," J. Micromech. Microeng. 11, 287–300 (2001).

ACKNOWLEDGMENTS

Supported by the Israel Science Foundation (ISF) Bikura Grant and by the Marie Curie Career Integration Grant (CIG).